Jumps in Electronic Conductance Due to Mechanical Instabilities

T. N. Todorov and A. P. Sutton

Department of Materials, Oxford University, OX1 3PH, United Kingdom
(Received 30 November 1992)

Using an exact single-particle scattering formalism we have carried out the first calculation of the conductance of a metallic contact, on the basis of a full dynamic simulation of the evolution of its atomic structure. We find that the contact area evolves discontinuously through a series of mechanical instabilities, which is reflected in a stepwise variation of the conductance also seen in recent experiments. Importantly, we find that the conductance is not simply proportional to the size of the contact and, therefore, the conductance *per atom* is not constant.

The scanning tunneling [1] and atomic force [2] microscopes have recently been adapted to produce a number of ingenious point contact experiments. The purpose of these experiments is to study the electrical conduction characteristics of a contact between a tip, often of nanometer dimensions, and a surface. The electronic conductance has been measured throughout the approach and formation of the contact [3,4], the growth of the contact [5], or while a contact is slid along the substrate surface [6]. During the approach and formation of the contact the electronic conductance is observed to jump discontinuously [3,4]. This has been attributed to the "jump-to-contact" phenomenon in which the tip-substrate system becomes mechanically unstable at a critical separation [7]. As the contact grows the conductance is found to increase in steps [5]. During sliding [6] the conductance variations are due to the periodic changes of the atomic topology of the contact.

In all previous theoretical treatments [8] of the conductance problem no account has been taken of the dynamical evolution of the atomic topology of the contact, while the evolution of the size and shape of the contact has been considered only via unrealistically simplified geometries.

In this Letter we report the first calculation of the evolution of the conductance of a metallic contact on the basis of a full dynamic simulation of its atomic structure. We find that the contact area evolves discontinuously through a series of mechanical instabilities, which is the origin of the stepwise variation of the conductance that is found in our simulations and that has already been seen in point contact measurements [5]. Moreover, we find that the conductance *per atom* in the contact varies during contact growth.

In our dynamic simulations a metallic tip is brought into contact with a substrate of the same metal and is then pulled off. The atomic interactions are described by an N-body potential [9] which has the form of a long-range Finnis-Sinclair potential [10]:

$$E = \varepsilon \left\{ \frac{1}{2} \sum_i \sum_{j \neq i} \left(\frac{a}{r_{ij}} \right)^n - c \sum_i \left[\sum_{j \neq i} \left(\frac{a}{r_{ij}} \right)^m \right]^{1/2} \right\}. \qquad (1)$$

Here, r_{ij} is the distance between atoms i and j, ε, m, and n are parameters that have been fitted to ten fcc metals in [9], and a is the respective fcc lattice constant. The dimensionless parameter c is determined by the equilibrium condition for the perfect fcc crystal. The potential is truncated at $r_{ij} = 2.001a$, which means that in a perfect fcc crystal there are 140 interacting neighbors to a given atom. As shown in [9] the *long range* interaction between the tip and substrate in Eq. (1) is a sum of inverse power pair potentials, $\sim 1/r^m$, which are van der Waals potentials if $m = 6$. As the tip approaches the surface this interaction is transformed smoothly into the full N-body Finnis-Sinclair form, thereby describing metallic bonding [9].

Previous simulations [11,12] of contact formation and fracture for a variety of fcc metals have all shown the same mechanical behavior at a given homologous temperature. Therefore, the choice of metal for the present model calculation is not critical, and the particular set of parameters chosen is that for iridium. Thus, $m = 6$, $n = 14$, $\varepsilon = 2.4489 \times 10^{-3}$ eV, $a = 0.384$ nm, and $c = 334.94$ [9].

Figure 1 shows the geometry and boundary conditions
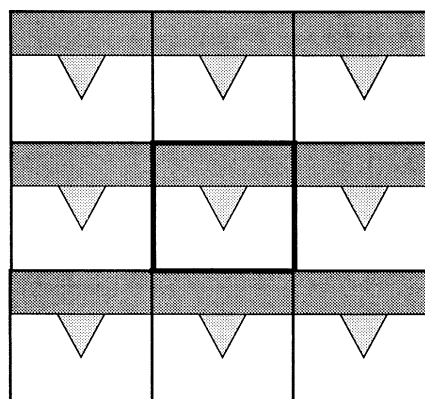
FIG. 1. Schematic illustration of the use of periodic boundary conditions to simulate tip-surface interactions. The emboldened cell is repeated in three orthogonal directions.

used to model the interaction between a paraboloidal tip and substrate [11,12]. The tip in the computational cell is attached to the underside of the slab. The slab comprises six (111) fcc planes and contains 1836 atoms. The tip, which has the same crystal structure and orientation as the slab, comprises initially eight (111) layers, and contains 207 atoms. The lowermost "layer" of the tip contains only 1 atom, while the layer above it contains 12 atoms, and the layer above that contains 19. By decreasing (increasing) the length of the cell normal to the slab the tip is moved closer to (further from) the upper side of the slab in the image cell below. In this way *all* atoms are treated dynamically, with no artificial interfaces between dynamic and static regions. The variation of the cell length is achieved by applying a homogeneous uniaxial strain to the contents of the cell. This strain localizes and becomes inhomogeneous naturally through the dynamical motion of the atoms. The Newtonian equations of motion are integrated via the velocity Verlet algorithm [13], and a Nosé-Hoover thermostat is applied [12] to all atoms in the cell to maintain the average temperature at 300 K. The time step is 10^{-14} s.

Initially the tip and slab are equilibrated for 1050 time steps, during which the tip is not interacting with the substrate below. The distance between the tip and the substrate below is then set to $2.007a$ (i.e., there is still no interaction between them at this separation) and the cell length normal to the slab is decreased at a rate of $0.0015a$ per time step for 2150 time steps. A significant contact area is established during this time. The tip is then pulled off the substrate by increasing the cell length at the same rate for 3000 time steps. The velocity of the tip, about 60 m/s, is small compared with the speed of sound in the material (4900 m/s). Therefore, although the velocity of the tip is much greater than is found in experiments (e.g., [5]), it is sufficiently small to allow the structure to reequilibrate between successive instabilities.

At each of the 5150 time steps of the dynamic simulation, following the initial equilibration, the set of atomic coordinates for the tip is used explicitly for computing the conductance of the respective configuration. In view of the size and duration of the simulation the conductance calculation must necessarily be a model calculation employing the simplest possible basis set which allows the relationship between atomic structure and metallic conduction to be traced. For this reason the electronic structure of the entire system is described by an orthonormal, nearest-neighbor, $1s$ tight-binding model with zero on-site energies, a band filling of one-half, and hopping integral scaling calculated analytically [14] for $1s$ orbitals on hydrogenic atoms. Thus the hopping integral H_{ij} between atoms i and j is given by

$$H_{ij} = A \frac{1 + \alpha z_{ij}}{1 + \alpha} \exp[\alpha(1 - z_{ij})], \tag{2}$$

where A is the hopping integral between nearest neighbors in the perfect crystal, α is a dimensionless constant

(in this calculation $\alpha = 4$), and z_{ij} is the distance between atoms i and j in units of the ideal nearest-neighbor separation. This hopping integral is truncated for $z_{ij} \geq \sqrt{2}$.

Periodic boundary conditions are not used for the conductance calculation. Instead, we consider a single tip between two semi-infinite crystals. The atomic positions within the tip are those given by the simulation. The distortion of the slabs in the simulation is negligible compared with that of the tip, as can be seen from Fig. 2. Therefore, in the conductance calculation the slabs above and below the tip are replaced by semi-infinite, perfect crystals, labeled 1 and 2, respectively. We imagine that the tip atoms are initially decoupled from each other and from the substrate atoms. We then couple the tip atoms to each other and to the substrate atoms by a coupling V, whose matrix elements have the functional form specified in Eq. (2). All on-site matrix elements of V are taken to be zero.

In a recent single-particle scattering theory formulation of the conductance problem [15], and in agreement with [16], the zero-voltage, zero-temperature elastic conductance g of the final, coupled system was shown to be given by

$$g = (2e^2/h)4\pi^2 \text{Tr}[\rho_1^0(E_F)t^\dagger(E_F)\rho_2^0(E_f)t(E_f)], \tag{3}$$

where $t(E) = V + VG^+(E)V$, E_F is the Fermi energy, and $\rho_1^0(E)$ and $\rho_2^0(E)$ are the density of states operators for the respective initial substrates and are given by

$$\rho_k^0(E) = (1/2\pi i)[G_k^{0-}(E) - G_k^{0+}(E)], \quad k = 1,2. \tag{4}$$

Here $G_1^{0\pm}(E)$ and $G_2^{0\pm}(E)$ are the Green's operators for the respective substrates in the initial, decoupled sys-
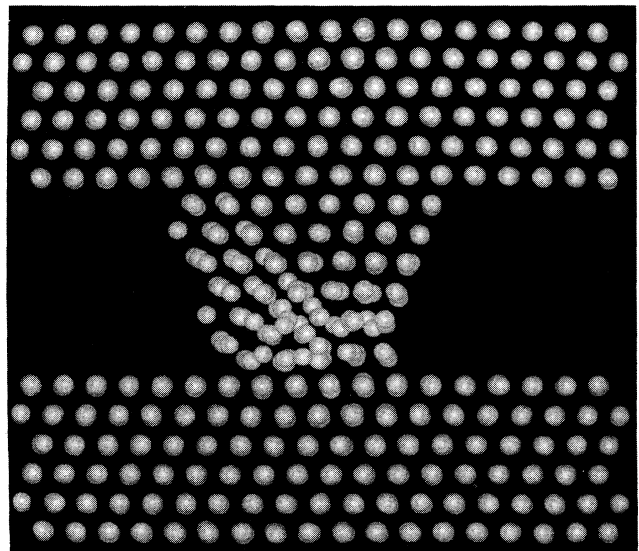
FIG. 2. A snapshot ($N = 2730$) of the dynamic simulation of the tip in contact with the slab below. Note that the distortions in the slab are small relative to those in the tip.

tem and $G^{\pm}(E)$ are the Green's operators for the final, coupled system. (Superscripts $+$ and $-$ correspond to retarded and advanced, respectively.)

The trace in Eq. (3) is taken in the orthonormal atomic $1s$ basis. The matrix elements of $G_1^{0\pm}(E)$ and $G_2^{0\pm}(E)$ are obtained by a method described in [15], and those of $t(E)$ by solving the Dyson matrix equation $[1 - V \times G^{0+}(E)]t(E) = V$. The matrix element $(G^{0+}(E))_{ij}$ of $G^{0+}(E)$ between atomic basis states i and j is given by $(G_1^{0+}(E))_{ij}$ if $i, j \in$ substrate 1, and $(G_2^{0+}(E))_{ij}$ if $i, j \in$ substrate 2; δ_{ij}/E if $i, j \in$ tip and zero otherwise.

Figure 3 shows the conductance (in units of $2e^2/h$) as a function of the iteration (time step) number N of the dynamic simulation, following the initial equilibration which occurs for $1 \leq N \leq 1050$. For $1050 < N \leq 3200$ the computational cell length is being decreased, whereas for $3200 < N \leq 6200$ it is being increased, at the rate specified earlier. Owing to the truncation of the hopping integral the conductance is zero until substrate atoms come within hopping range of tip atoms. This happens at $N = 1784$. After that the conductance rises as the bonds between the single atom at the bottom of the tip and its three neighbors in the substrate below strengthen. For $1940 \leq N \leq 2090$, when, apart from thermal fluctuations, there is a stable single atom contact, the conductance settles at a value of 0.93 ± 0.05.

Between $N \approx 2100$ and $N \approx 2230$ we see the first mechanical instability in which the single atom at the base of the tip is incorporated into the layer above, and the number of layers in the tip is reduced by one. The system becomes unstable in the sense that, once induced, the structural rearrangement persists even if the change in cell length is suspended. Now there are 13 atoms of the tip in direct contact with the slab. During the rearrangement the conductance undergoes a sharp increase and for $2300 \leq N \leq 2600$ it settles at a value of 9.0 ± 0.3, giving a conductance per atom of 0.69 ± 0.02.
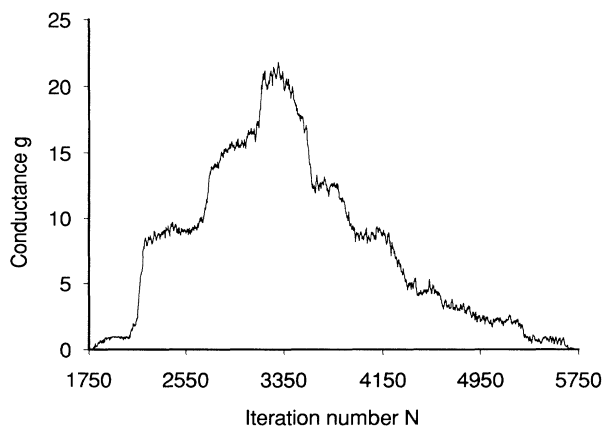
FIG. 3. The conductance (in units of $2e^2/h$) vs the iteration number N of the dynamic simulation throughout the formation and breaking of the contact.

The next instability occurs between $N \approx 2650$ and $N \approx 2750$. The number of layers in the tip is again reduced by one, and the number of tip atoms in direct contact with the slab becomes 25. Once again the conductance undergoes a sharp increase and for $2800 \leq N \leq 3000$ it settles at a value of 15.20 ± 0.5, yielding a conductance per atom of 0.61 ± 0.02. We see the onset of one further reduction in the number of tip layers just before the cell length starts being increased at $N = 3200$.

Between successive sharp increases, the conductance exhibits some small variation. This variation is due to two factors: (i) thermal vibrations giving rise to random fluctuations in the conductance, and (ii) the growing compressive force promoting improved registry between the tip and substrate atoms, which leads to a further slight increase in the conductance between jumps.

The above observations indicate that the main factor governing the conductance is the number of tip atoms in direct contact with the substrate. However, the conductance does not vary linearly with this number. The variation in the conductance per atom is due to two independent factors. First, even with a perfect geometry (i.e., when all bond lengths are equal to that in the perfect crystal), the conductance for a given contact area depends on the shape of the rest of the tip. Second, there is interference between the single-atom contacts that make up a multiatom contact. This phenomenon is best illustrated by a calculation discussed in [15] in which, using the same tight-binding model as here, we showed that in the limit of an infinite ideal contact between two fcc (111) semi-infinite perfect crystals, the conductance per atom is 0.81 (in units of $2e^2/h$), whereas the conductance of an ideal single-atom contact between these semi-infinite crystals is unity.

Between $N = 3200$ and $N = 6200$ the tip is being pulled off the slab. As in our earlier simulations [11,12] fracture does not take place between the lowermost layer of the tip and the slab, but through the formation of a neck within the tip. Mechanical instabilities are induced during the elongation of the tip, each of which results in the formation of a new layer in the neck region. This is reflected in sharp decreases in the conductance at $N \approx 3500$, 3900, and 4300. Beyond $N \approx 4500$ the neck becomes highly disordered and without a well defined layer structure. Just before fracture, between $N \approx 5300$ and $N \approx 5600$, the neck reduces to a single-atom width. Finally, when fracture occurs, a pile of tip atoms is left behind on the slab.

We have found that once mechanical contact has been established, the value of the hopping decay rate α [see Eq. (2)] modulates the size of the thermal fluctuations in the conductance, but does not affect the general features of the conductance curve.

We emphasize that the mechanical instabilities, which manifest themselves as the generation or loss of tip layers, and the resulting discontinuities in the conductance, are a general feature of atomic scale contacts, even though the

particular abrupt rearrangements and conductance jumps depend on the initial structure of the tip.

In conclusion, first we have shown that an atomic scale metallic contact evolves through abrupt structural changes, which lead to abrupt changes in its conductance. Second, the main factor controlling the conductance is the area of the contact while perturbations of the internal structure of the tip are of secondary importance. Finally, the conductance does not vary linearly with the number of atoms in the contact.

[1] G. Binnig, H. Rohrer, Ch. Gerber, and E. Weibull, Appl. Phys. Lett. **40**, 178 (1982); Phys. Rev. Lett. **49**, 57 (1982).

[2] G. Binnig, C. F. Quate, and Ch. Gerber, Phys. Rev. Lett. **56**, 930 (1986).

[3] J. K. Gimzewski and R. Möller, Phys. Rev. B **36**, 1284 (1987).

[4] U. Dürig, O. Züger, and D. W. Pohl, Phys. Rev. Lett. **65**, 349 (1990).

[5] C. J. Muller, J. M. van Ruitenbeek, and L. J. de Jongh, Phys. Rev. Lett. **69**, 140 (1992).

[6] J. D. Todd and J. B. Pethica, J. Phys. Condens. Matter **1**, 9823 (1989).

[7] J. B. Pethica and A. P. Sutton, J. Vac. Sci. Technol. A **6**, 2490 (1988).

[8] J. Ferrer, A. Martin-Rodero, and F. Flores, Phys. Rev. B **38**, 10113 (1988); N. D. Lang, Phys. Rev. B **36**, 8173 (1987); E. Tekman and S. Ciraci, Phys. Rev. B **39**, 8773 (1989); **40**, 8559 (1989); S. Ciraci and E. Tekman, Phys. Rev. B **40**, 11969 (1989); E. Tekman and S. Ciraci, Phys. Rev. B **42**, 9098 (1990); **43**, 7145 (1991); S. Ciraci, Ultramicroscopy **42-44**, 16 (1992); S. Ciraci, E. Tekman, M. Gökçedag, I. P. Batra, and A. Baratoff, Ultramicroscopy **42-44**, 163 (1992).

[9] A. P. Sutton and J. Chen, Philos. Mag. Lett. **61**, 139 (1990).

[10] J. E. Sinclair and M. W. Finnis, Philos. Mag. A **50**, 45 (1984).

[11] A. P. Sutton and J. B. Pethica, J. Phys. Condens. Matter **2**, 5317 (1990).

[12] A. P. Sutton, J. B. Pethica, H. Rafii-Tabar, and J. A. Nieminen, in *Electron Theory in Alloy Design*, edited by D. G. Pettifor and A. H. Cottrell (Institute of Materials, London, 1992), Chap. 7.

[13] M. P. Allen and D. J. Tildesley, *Computer Simulation of Liquids* (Oxford Univ. Press, Oxford, 1987).

[14] N. F. Mott, *Metal-Insulator Transitions* (Taylor & Francis, London, 1990), p. 9, Eq. (11).

[15] T. N. Todorov, G. A. D. Briggs, and A. P. Sutton (to be published).

[16] J. B. Pendry, A. B. Prêtre, and B. C. H. Krutzen, J. Phys. Condens. Matter **3**, 4313 (1991).

FIG. 2. A snapshot ($N = 2730$) of the dynamic simulation of the tip in contact with the slab below. Note that the distortions in the slab are small relative to those in the tip.